JOC The Journal of Organic Chemistry

Article

pubs.acs.org/joc

Aerobic Palladium(II)-Catalyzed Dehydrogenative Heck Reaction in the Synthesis of Pyrenyl Fluorophores. A Photophysical Study of β-Pyrenyl Acrylates in Solution and in the Solid State

Michał Piotrowicz,[†] Janusz Zakrzewski,*[,†] Rémi Métivier,*[,‡] Arnaud Brosseau,[‡] Anna Makal,[§] and Krzysztof Woźniak[§]

[†]Faculty of Chemistry, Department of Organic Chemistry, University of Łódź, Tamka 12, 91-403 Łódź, Poland

[‡]PPSM, ENS Cachan, CNRS, UniverSud, 61 avenue President Wilson, 94230 Cachan, France

[§]Biological and Chemical Research Centre, Department of Chemistry, University of Warsaw, Żwirki i Wigury 101, 02-089 Warszawa, Poland

Supporting Information

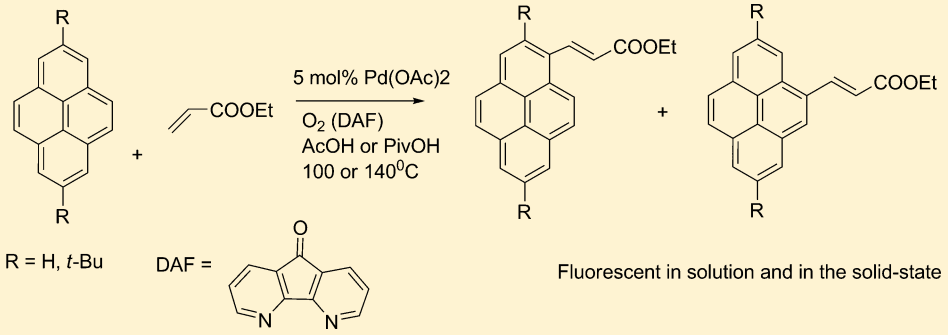

ABSTRACT: An aerobic dehydrogenative Heck reaction of pyrene (**1a**) and 2,7-di-*tert*-butylpyrene (**1b**) with ethyl acrylate is reported. The reaction is catalyzed by a $Pd(OAc)_2$/4,5-diazafluoren-9-one (DAF) system and takes place in acetic or pivalic acid as solvents at 110−130 °C. The reaction of **1a** afforded a 6:1 mixture of C-1- and C-4-alkenylated pyrenes (**2a** and **3a**, respectively) in 71% yield. In the case of **1b**, only a C-4-substituted product (**3b**) was formed in 46% yield. Compounds **2a** and **3a,b** exhibited fluorescence in solution and in the solid state. In chloroform and THF solution the fluorescence maxima were in the range of 440−465 nm, and quantum yields decreased in the order **2a** > **3a**> **3b**. In the solid state, **3a,b** showed blue-green fluorescence (Φ_F = 0.26 and 0.14, respectively), whereas **2a** emitted yellow-green fluorescence) (Φ_F = 0.35). Besides blue-emitting monomers, the presence of green-emitting aggregated species (preformed dimers) in the crystals of **3a,b** and red-emitting dynamic excimers in the crystals of **2a** has been demonstrated. Single-crystal X-ray diffraction analyses of **2a** and **3b** confirmed π-stacking of pyrenyl moieties in the crystals of the former and the absence of stacking in the crystals of the latter compound.

1. INTRODUCTION

Pyrene and its derivatives are important and thoroughly investigated organic fluorophores that have found various applications in molecular electronics and photovoltaic cells and as fluorescent probes and sensors.[1−6] Alkenylpyrenes have been used as monomers for the synthesis of polymers containing fluorescent groups attached to the polymer backbone[7] and as probes to monitor polymerization.[8] It has been found that the conjugation of alkenyl groups with the pyrenyl moiety strongly influences the electronic structure and luminescent properties of such compounds.[9−11] Until now, a general route to alkenylpyrenes has been a classical cross-coupling reaction starting from corresponding bromo- or iodopyrenes.[12−15]

In this paper, we present a preliminary report on a simple, efficient, atom- and step-economical route to alkenylpyrenes having an ester group at the alkenyl group (pyrenyl acrylates) based on dehydrogenative alkenylation (dehydrogenative Heck reaction, i.e., DHR or the Fujiwara−Moritani reaction)[16] of pyrene with ethyl acrylate. We have also studied the photophysical properties of these compounds in solution and in the solid state.

2. RESULTS AND DISCUSSION

2.1. Dehydrogenative Heck Reaction (DHR). DHR constitutes a class of dehydrogenative cross-coupling (DCC) reactions which are considered to be one of the most challenging topics in modern organic synthesis.[17−24] DHR is of special interest because π-conjugated alkenylated arenes display interesting electronic properties and are versatile

Received: November 17, 2014
Published: February 2, 2015

DOI: 10.1021/jo502619k
J. Org. Chem. 2015, 80, 2573−2581

Scheme 1. Aerobic DHR of Pyrene and 2,7-Di-*tert*-butylpyrene with Ethyl Acrylate

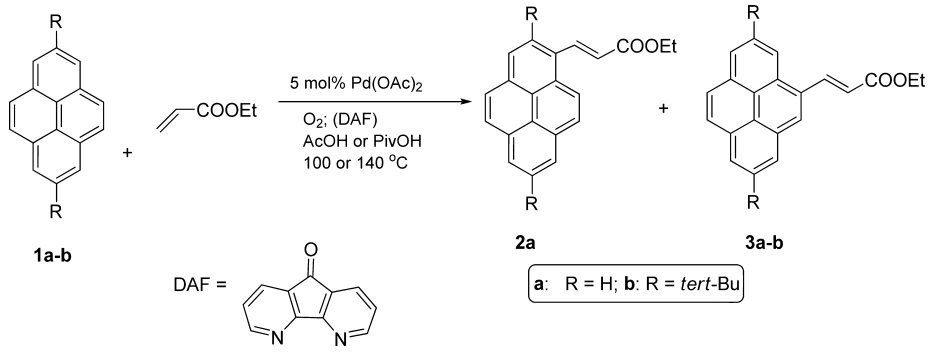

building blocks in organic synthesis. Despite their simplicity and environmentally friendly character, the DCC reactions found so far have demonstrated only little use in structural modifications of pyrene, with reported examples being limited to arylation and borylation[25−28]

In our first attempts, we applied the experimental conditions described previously for alkenylation of ferrocene,[29] i.e., palladium(II) acetate as catalyst, 4,5-diazafluoren-9-one (DAF) as an auxiliary ligand, molecular oxygen under atmospheric pressure as the oxidant, and acetic acid as the solvent (Scheme 1). However, by performing this reaction at 70 °C we obtained only a trace amount of alkenylated pyrenes, which is in line with the lower nucleophilic reactivity of pyrene than ferrocene.

Better results were obtained when the reaction was performed at 100 °C (Table 1). In the absence of DAF the reaction afforded mixtures of **2a** and **3a** in the ratio of 3:1 to ∼2:1. The replacement of air by O_2 at atmospheric pressure brought an approximately 2-fold increase in the yield (Entries 1−2). The addition of DAF only slightly influenced the yield but significantly changed the regioisomer ratio from ∼2:1 to ∼6:1 (Entries 2 and 3). The best yield (71%) was obtained after 6 h of heating, and longer reaction times did not improve this value. The regioisomer ratio was the same as that found after 1.5 h of heating.

Table 1. Dehydrogenative Alkenylation of 1a with Ethyl Acrylate[a]

entry	conditions	yield (**2a** + **3a**)[b] (%)	**2a**:**3a**[c]
1	air (1 atm), 2.5 h	30	75:25
2	O_2 (1 atm), 1.5 h	59	69:31
3	O_2 (1 atm), 1.5 h, 5 mol % DAF	54	86:14
4	O_2 (1 atm), 4 h, 5 mol % DAF	60	83:17
5	O_2 (1 atm), 6 h, 5 mol % DAF	71	84:16

[a]Molar ratio pyrene/acrylate 3:1; temperature 100 °C. [b]Isolated yields. [c]Determined from ^{1}H NMR spectra via integration of the olefinic protons signals (see Figure 1).

The major reaction product **2a** was isolated from the reaction mixture by fractional crystallization and identified by a comparison with a sample obtained via the classical Heck reaction from 1-bromopyrene and ethyl acrylate.[10] However, we were unable to isolate **3a** in pure form. Therefore, we synthesized this compound via Heck reaction[10] from 4-bromopyrene[30] (Scheme 2) and demonstrated that the ^{1}H NMR spectrum of the mixture of products is identical with the spectrum of a 6:1 mixture of **2a** and **3a** prepared from pure components (Figure 1).

The formation of the mixture of products of alkenylation at 1- and 4-position from pyrene prompted us to see how this reaction proceeds with 2,7-di-*tert*-butylpyrene **1b**. $Pd(OAc)_2$-catalyzed DHRs are believed to involve electrophilic metalation of arene by "$PdOAc^+$", and it is known that some electrophilic substitutions of this compound (bromination, nitration) occur at the 1-position,[31,32] whereas in the other (formylation, Friedel−Crafts acylation) electrophile attacks the 4-position.[33]

Our first attempts to perform DHR of **1b** with ethyl acrylate, under the same conditions as for pyrene, failed, presumably because of the very limited solubility of this compound in acetic acid. Therefore, we replaced acetic acid with pivalic acid (PivOH), in which **1b** is more soluble and has a higher boiling point, enabling a reaction at a higher temperature at atmospheric pressure. Furthermore, PivOH proved to be a solvent of choice in the DHRs of chromones and coumarins[34,35] as well as in dehydrogenative arene−arene coupling.[36]

The reaction of **1b** with ethyl acrylate in PivOH was carried out at 130 °C and afforded **3b** in 46% isolated yield. Although the yield was moderate, the product was very easily isolated by column chromatography, and most of the unreacted di-*tert*-butylpyrene could be recovered and recycled. We did not optimize the reaction conditions. Compound **3b** was fully characterized by NMR, IR, and elemental analysis, and its structure was confirmed by single-crystal X-ray diffraction (vide infra).

The observed selectivity of DHR of **1b** for substitution at the 4-position is similar to those reported for formylation and

Scheme 2. Synthesis of 3a

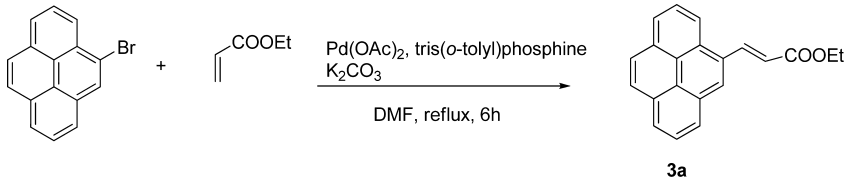

DOI: 10.1021/jo502619k
J. Org. Chem. 2015, 80, 2573−2581

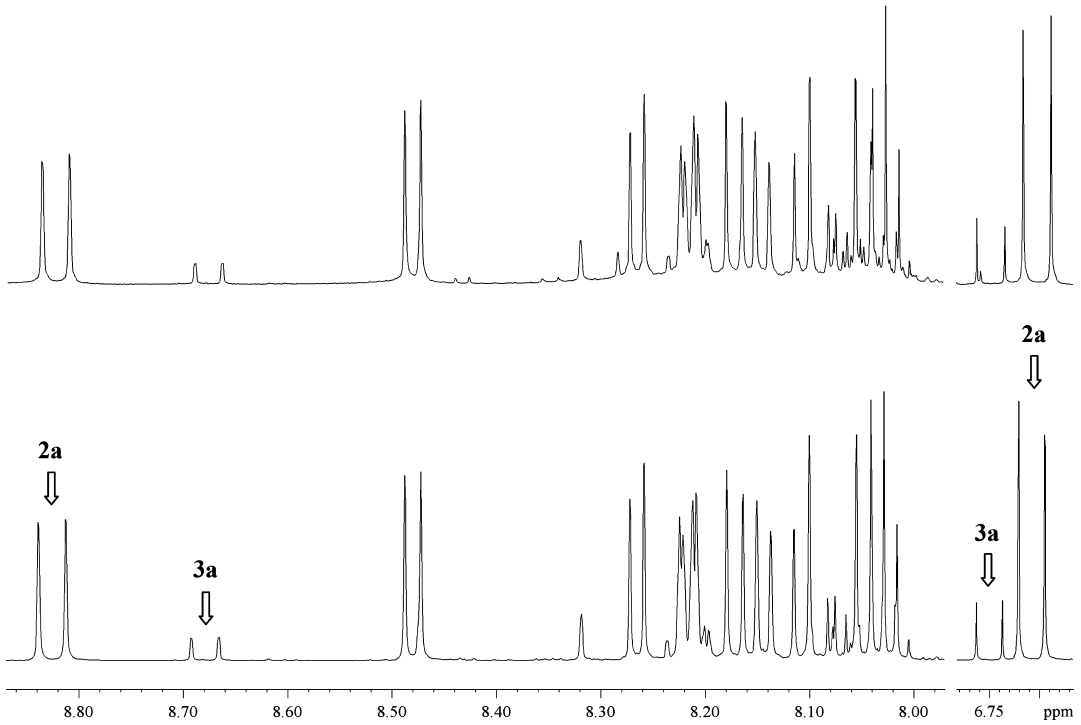

Figure 1. ^{1}H NMR spectra (600 MHz, $CDCl_3$, aromatic and olefinic proton region) of the mixture of products of DHR of pyrene with ethyl acrylate (top) and the 6:1 mixture of **2a** and **3a** (bottom).The arrows show signals of the olefinic protons of both compounds.

Friedel–Crafts acylation and may be attributed to the steric effect of bulky *tert*-butyl groups.

2.2. Photophysical Study of 2a and 3a,b in Solution. We have studied steady-state absorption, fluorescence excitation, and emission spectra of **2a** and **3a,b** in various solvents (see the Supporting Information). The spectra in $CHCl_3$ and THF solutions are shown in Figure 2. Compiled spectroscopic data in solution are gathered in Table 2.

The lowest energy absorption band of the studied compounds appears at 327–368 nm and increases in the order **3a** < **3b** < **2a**. This may suggest that π-conjugation of the acrylic chain with the pyrenyl moiety increases in the same order. On the other hand, the maximum wavelengths of fluorescence emission in $CHCl_3$ are in the order **2a** < **3a** < **3b**. Consequently, **2a** shows a relatively small Stokes shift (4450 cm^{-1}) in comparison to those of **3a** and **3b** (7200 and 6650 cm^{-1}, respectively). This significant difference between **2a** and **3a,b** reflects a variable conjugation configuration due to the different substitution mode on the pyrenyl backbone. The same trends are observed in THF solution, with only slight changes as compared to $CHCl_3$, except the fluorescence quantum yield which is multiplied by a factor 2 and reaches almost unity in the case of **2a** in THF.

We also performed a time-resolved study of fluorescence of **2a** and **3a,b** in solution. The aerated samples were excited at 330 nm, and fluorescence decays were observed at wavelengths corresponding to the maximum of emission. The fluorescence decays recorded in $CHCl_3$ and in THF (Figure 3) show similar curves for **3a** and **3b**, whereas the fluorescence of **2a** decays much more quickly.

The fitting of the fluorescence decays reveals, in most cases, biexponential behavior, thus signaling the contribution of two emitting species, major (≥92%) and minor (≤8%) ones, probably due to different conformers (Table 3). Monoexponential decay was observed for **3b** in THF. As observed

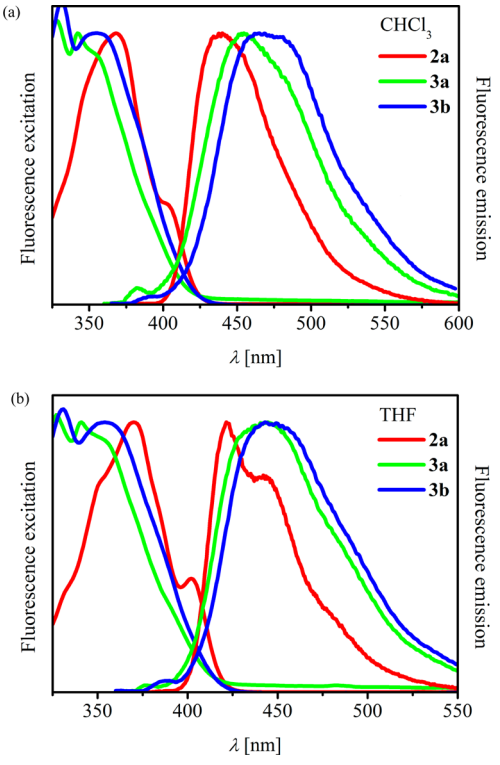

Figure 2. Normalized fluorescence excitation and emission spectra of **2a** and **3a,b** in $CHCl_3$ (a) and THF (b). Concentration: 10^{-6} M.

qualitatively, the lifetime of the major component increased in the order **2a** < **3b** ~ **3a** (for the minor component this was **2a** < **3a**). The fluorescence lifetimes were significantly longer in a more polar solvent such as THF (ε = 7.5; μ = 1.5 D, as compared with ε = 4.8; μ = 1.15 D for $CHCl_3$). The calculation

DOI: 10.1021/jo502619k
J. Org. Chem. 2015, 80, 2573–2581

Table 2. Steady-State Absorption and Emission Data for 2a and 3a,b in Solution

compd	solvent	absorption[a] λ_{max} (nm)	emission[b] λ_{max} (nm)	Φ_F[c]
2a	$CHCl_3$	368	440	0.42
2a	THF	372, 402	422	0.98
3a	$CHCl_3$	328, 342	454	0.36
3a	THF	327, 341	444	0.71
3b	$CHCl_3$	331, 355	465	0.31
3b	THF	331, 354	443	0.54

[a]Concentration: 10^{-5} M. [b]Concentration: 10^{-6} M. [c]Measured for aerated solutions using quinine bisulfate in 1 M sulfuric acid as a standard. We did not observe any change in emission intensity after bubbling argon in the solutions.

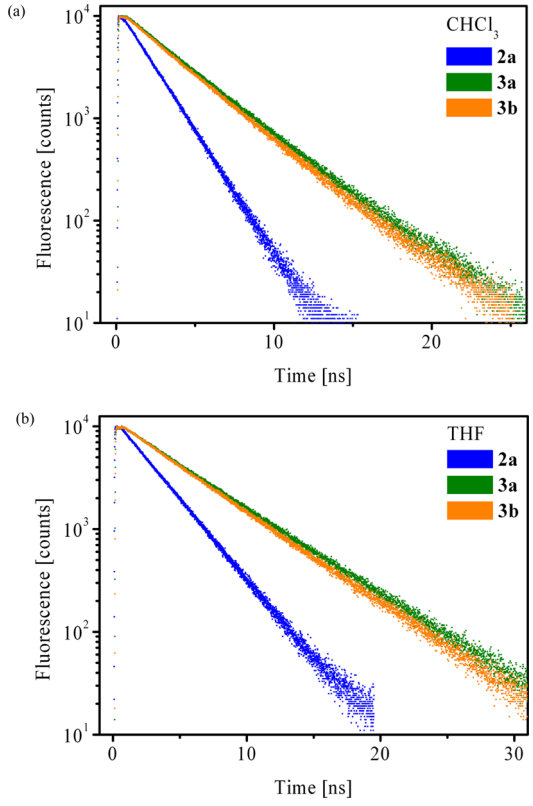

Figure 3. Fluorescence decays of **2a** and **3a,b** in $CHCl_3$ and THF.

Table 3. Time-Resolved Fluorescence Emission Data for 2a and 3a,b in Solution[a]

compd	solvent	τ_i (ns) (a_i)	$k_r/10^8$ (s^{-1})	$k_{nr}/10^8$ (s^{-1})
2a	$CHCl_3$	1.78 (0.96); 0.25 (0.04)	2.4	3.3
2a	THF	2.76 (0.97); 0.56 (0.03)	3.6	0.07
3a	$CHCl_3$	3.62 (0.92); 1.52 (0.08)	1.0	1.8
3a	THF	5.14 (0.95); 2.38 (0.05)	1.4	0.6
3b	$CHCl_3$	3.45 (0.92); 1.23 (0.08)	0.9	2.0
3b	THF	4.80 (1.00)	1.1	1.0

[a]$k_r = \Phi/\langle\tau\rangle$; $k_{nr} = (1 - \Phi)/\langle\tau\rangle$, where $\langle\tau\rangle = (a_1\tau_1^2 + a_2\tau_2^2)/(a_1\tau_1 + a_2\tau_2)$; τ_i: decay times. a_i: pre-exponential factors.

of radiative and nonradiative deactivation rates (k_r and k_{nr}), based on averaged lifetimes and fluorescence quantum yields (Tables 2 and 3), leads to the following conclusions that, on the one hand, a much higher k_r was found for **2a** than for **3a,b** ($3.0 \pm 0.6 \times 10^8$ s^{-1} vs $1.1 \pm 0.3 \times 10^8$ s^{-1}, respectively); on the other hand, k_{nr} is very sensitive to the solvent nature for all studied compounds, with a clear decrease of k_{nr} in THF as compared to $CHCl_3$, which means that nonradiative deactivation channels are considerably hampered in THF.

2.3. Photophysical Study of 2a and 3a,b in the Solid State. The fluorescence excitation and emission spectra of **2a** and **3a,b** in the solid state (powders) are shown in Figure 4. A comparison of the spectra recorded in $CHCl_3$ solution and in the solid state is displayed in Figure 5.

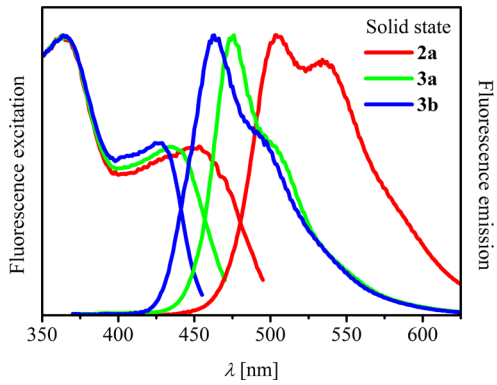

Figure 4. Fluorescence excitation and emission spectra of **2a** and **3a,b** in the solid state.

Excitation spectra in the solid state are characterized by two main bands. The first band maximum is located in the 425−450 nm range, in the order **3b** (425 nm) < **3a** (435 nm) < **2a** (450 nm), whereas the second band maximum is rather identical for all compounds, ca. 360−365 nm (Figure 4). Since this second excitation band corresponds more or less to the main band observed in solution (Figure 5), one can attribute it to some monomer contribution. Therefore, the first excitation band, missing in solution and red-shifted toward lower energy, can be tentatively attributed to an aggregated state in the solid state, such as preformed dimers in the ground state. Then, in all three compounds, both monomer and aggregate emissions are foreseen.

The fluorescence emission spectra of **2a** and **3a,b** in the solid state are strongly red-shifted, as compared to their solution counterparts. It is worth noting that the emission spectra of **3a,b** in the solid state overlap (at least partially) their corresponding emission spectra in $CHCl_3$ solution. Conversely, in the case of **2a**, the overlap between solid state and solution emission spectra is rather limited. As a consequence, based on emission spectra considerations, the monomer contribution is expected to be more pronounced for **3a,b** than for **2a**.

Fluorescence decay profiles of **2a** and **3a,b**, displayed in Figure 6, were determined at various monitoring wavelengths in order to gain further insight into excited state dynamics that contribute to emissive decays (Table 4).

Generally, for all studied compounds, complex and multi-exponential decays were observed revealing several emitting species (conformers, locally excited and intramolecular charge-transfer states, etc.) displaying distinct fluorescence spectra. The species having the longest lifetimes displayed red-shifted emission. A striking difference in the photophysical behavior of **2a** and that of **3a,b** was that the former compound showed a component rising rapidly after the laser pulse and emitting at 570−640 nm, which could be assignable to the dynamic solid-state excimer. It is now well established that such excimers can be efficient emitters.[37−40]

DOI: 10.1021/jo502619k
J. Org. Chem. 2015, 80, 2573−2581

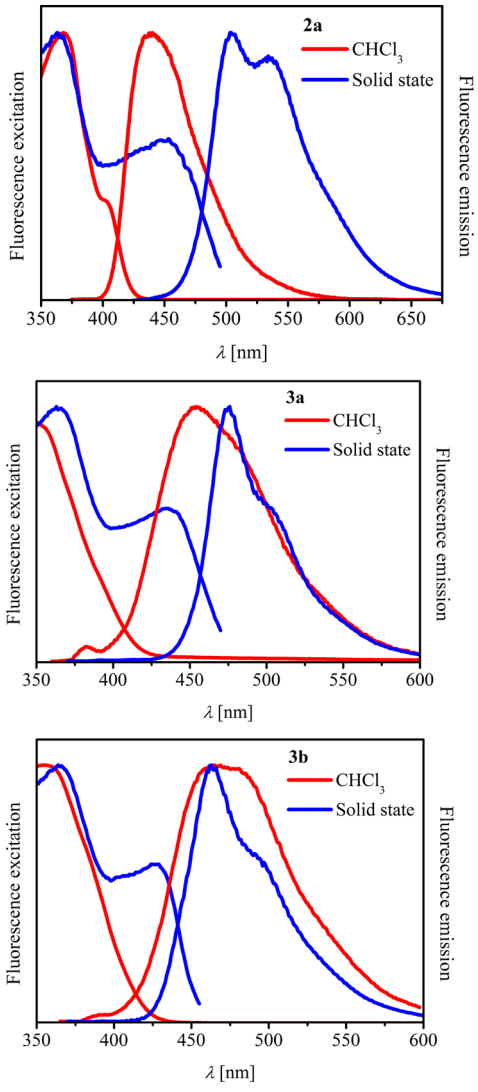

Figure 5. Comparison of solution- and solid-state fluorescence excitation and emission spectra of **2a** and **3a**,**b**.

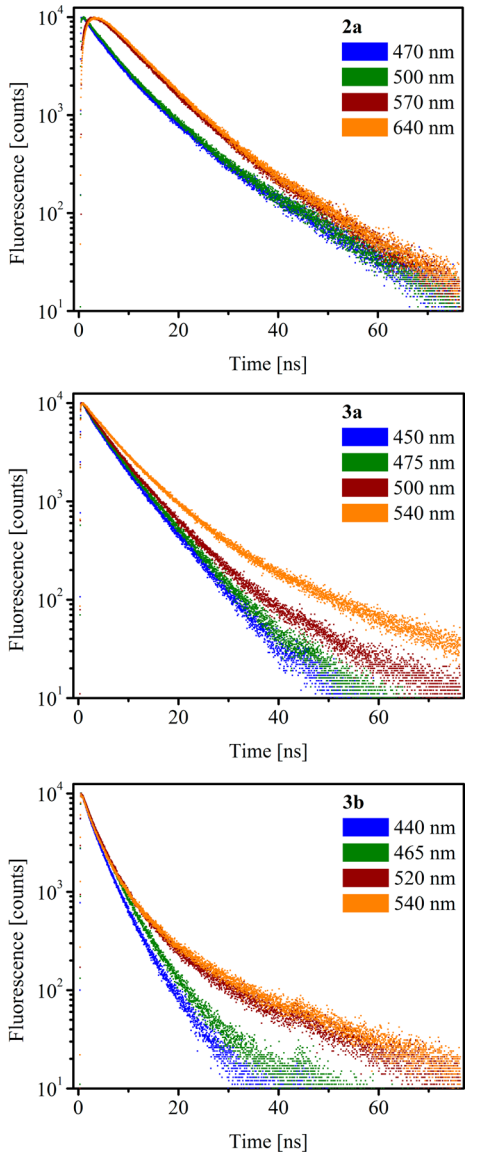

Figure 6. Fluorescence decays of **2a** and **3a**,**b** in the solid state.

For all of the studied compounds, the fluorescence decay curves show a strong wavelength dependence, and their general behavior is far from simple monoexponential kinetics. In the case of compounds **3a**,**b**, a rather long component contribution appears in the fluorescence decays when the emission wavelength increases (at λ_{em} > 500 nm, see Figure 5b,c). Most interestingly, in the case of **2a**, at shorter emission wavelengths (λ_{em} = 470−500 nm) the fluorescence decays with a multiexponential manner, whereas at longer emission wavelengths (λ_{em} = 570−640 nm) a rise time becomes much apparent within the first 5 ns of the fluorescence curves, which is followed by a decay period in the 5−80 ns time interval. In this latter situation, the presence of such a rise time in the red part of the emission spectrum is a convincing signature of dynamic excimer formation.

Appropriate global fitting analysis using a discrete multiexponential decay model which takes into account the full set of decay curves of a given compound provides additional information on the intimate excited state mechanisms which take place in the solid state. The corresponding decay parameters are compiled in Table 4.

For compound **2a**, the fluorescence decays can be satisfactorily fitted with a sum of four exponentials. Two short components (τ_1 = 1.2 ns and τ_2 = 3.4 ns) appear as decay contributions for λ_{em} = 470−500 nm and as rise times for λ_{em} = 570−640 nm. An intermediate decay time (τ_3 = 6.7 ns) shows an increased contribution to the fluorescence decays as the emission wavelength increases. Moreover, it is important to highlight that its pre-exponential factor corresponds quite well to the sum of the rising components at λ_{em} = 570−640 nm: $a_3 = -(a_1 + a_2)$. Indeed, for a homogeneous population of excimer-forming species the time evolution of the fluorescence intensities of the monomer and the excimer following a laser-pulse excitation is expected to be a sum of two exponentials and a difference of two exponentials, respectively.[6] Consequently, the first three components, τ_1, τ_2, and τ_3, can be assigned to a population of pyrenyl monomers which can form dynamic excimers within the time of their excited state and emit efficiently in the red part of the spectrum (570−640 nm). The need for two short times (τ_1 and τ_2) to obtain a satisfactory fitting of the rise time is probably due to several monomer configurations or spatial arrangements within the crystal lattice,

DOI: 10.1021/jo502619k
J. Org. Chem. 2015, 80, 2573−2581

Table 4. Time-Resolved Fluorescence Emission Data for 2a and 3a,b in the Solid State[a]

	λ_{em}[b]	τ_1 (a_1; f_1)[c]	τ_2 (a_2; f_2)[c]	τ_3 (a_3; f_3)[c]	τ_4 (a_4; f_4)[c]
2a	470		3.4 (0.26; 0.13)	6.7 (0.59; 0.55)	14.8 (0.15; 0.32)
	500		3.4 (0.16; 0.07)	6.7 (0.69; 0.62)	14.8 (0.15; 0.31)
	570	1.2 (−1.63; −0.08)	3.4 (−1.28; −0.19)	6.7 (3.45; 0.98)	14.8 (0.45; 0.29)
	640	1.2 (−5.33; −0.10)	3.4 (−5.02; −0.26)	6.7 (10.12; 1.05)	16.6 (1.24; 0.32)
3a	450	2.7 (0.33; 0.16)	6.9 (0.67; 0.83)	20.7 (<0.01; 0.01)	
	475	2.7 (0.26; 0.12)	6.9 (0.73; 0.85)	20.7 (0.01; 0.03)	
	500	2.7 (0.22; 0.09)	6.9 (0.75; 0.81)	20.7 (0.03; 0.10)	
	540	2.7 (0.07; 0.02)	6.9 (0.84; 0.73)	20.7 (0.09; 0.24)	
3b	440	1.8 (0.54; 0.32)	4.5 (0.45; 0.65)	19.5 (<0.01; 0.02)	
	465	1.8 (0.41; 0.22)	4.5 (0.58; 0.73)	19.5 (0.01; 0.05)	
	520	1.8 (0.44; 0.21)	4.5 (0.52; 0.60)	19.5 (0.04; 0.19)	
	540	1.8 (0.48; 0.22)	4.5 (0.47; 0.53)	19.5 (0.05; 0.25)	

[a]Decay parameters obtained for a global analysis of the full set of curves, for each compound, providing $\chi^2_R < 1.2$. [b]λ_{em} in nm. [c]τ_i in ns. f_i are the intensity fractions calculated by using the following equation: $f_i = a_i\tau_i/\Sigma a_j\tau_j$.

thus leading to excimer formation. Finally, the longer decay component (τ_4 = 14.8−16.6 ns) exists at all emission wavelengths and its contribution to fluorescence intensity remains almost constant whatever the λ_{em} (f_4 = 0.29−0.32). Then this long component may correspond to a fraction of molecules in a preformed aggregation state (also called the "preformed excimer" in the ground state), as is highlighted by the low energy band in the excitation spectra in the solid state (see the discussion above).

For compounds **3a,b**, three decay times are necessary to fit the fluorescence decays at all emission wavelengths. The first two decay components (τ_1 = 2.7 ns and τ_2 = 6.9 ns for compound **3a**; τ_1 = 1.8 ns and τ_2 = 4.5 ns for compound **3b**) correspond to the vast majority of emitting species ($a_1 + a_2$ > 91−95% for **3a** and **3b**, respectively), and even contribute to most of the fluorescence intensity ($f_1 + f_2$ > 75% for **3a**−**b**). Additionally, their contributions decrease for the longest emission wavelengths. Therefore, these two decay components can safely be assigned to several populations of blue-emitting monomers. The last decay component (τ_3 = 20.7 ns for compound **3a**; τ_3 = 19.7 ns for compound **3b**) corresponds to a minor proportion of emitting species (a_3 < 9%; f_3 < 25% for **3a**−**b**) with increasing contributions when λ_{em} increases, which may reflect the presence of a small fraction of preformed aggregated molecules in the solid state, mostly emitting in the green region of the spectrum (500−540 nm).

The color of the light by emitted **2a** and **3a**−**b** is shown in the CIE chromaticity diagram (Figure 7), The CIE chromacity coordinates along with the emission quantum yields are gathered in Table 5.

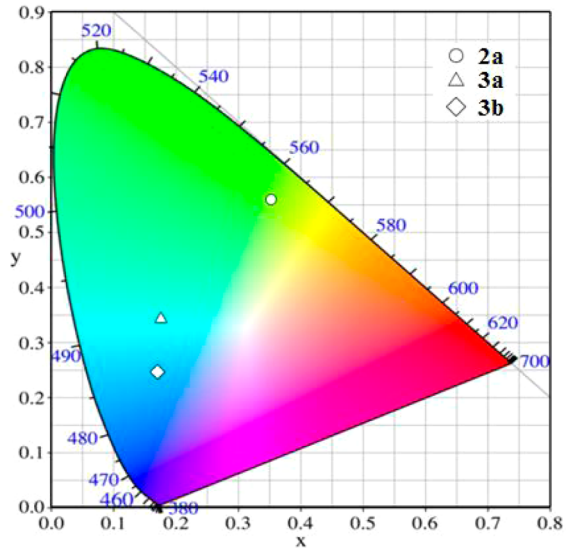

Figure 7. CIE chromaticity diagram for compounds **2a** and **3a,b**.

Table 5. Solid-State Fluorescence Quantum Yields (Φ) and CIE Chromaticity Coordinates (*x*,*y*) for Compounds 2a and 3a,b

compd	Φ	*x*	*y*
2a	0.35	0.35	0.56
3a	0.26	0.18	0.34
3b	0.14	0.17	0.24

3. SINGLE-CRYSTAL X-RAY DIFFRACTION STUDY OF 2A AND 3B

3.1. Molecular Structures. The molecular structures of **2a** and **3b** are shown in Figure 8.

The pyrene moiety is essentially planar in both structures, the dihedral angles around the central C15−C16 bond departing from 180° by less than 4° (Table 6). The side chain in **2a** is almost exactly coplanar with the pyrene moiety (the rotation of the C18 from the pyrene moiety is around 4°). On the other hand, the side chain in **3b** is slightly bent out of the pyrene plane, with C18 rotated by ∼26°. The C═C bonds in both compounds are almost coplanar with the C═O groups (dihedral angles C17−C18−C19−O1 equal to 177° for **2a** and 172° for **3b**). The C1−C17 bond in **2a** is shorter than the analogous bond (C6−C17) in **3a** (1.463(2) vs 1.473(2) Å), whereas the ethylenic (C17−C18) bond is longer in **2a** than in **3b** (1.336(2) vs 1.327(2) Å). This suggests a more efficient conjugation of the acrylate chain with the pyrenyl moiety in **2a**, which is consistent with our previous discussion based on spectroscopic data (see above, section 2.2).

3.2. Crystal Packings. Despite possessing similar molecular structures, compounds **2a** and **3b** show very different crystal packing and different sets of intermolecular interactions.

In the case of **2a**, the $\pi-\pi$ stacking is a dominant intermolecular interaction. The molecules of **2a** form infinite stacks of identically oriented molecules in the [100] direction (Figure 9a). The shortest distances are between the carbon atoms constituting a "backbone" of the molecule, including the C atoms of the C═C double bond of the substituent. The

DOI: 10.1021/jo502619k
J. Org. Chem. 2015, 80, 2573−2581

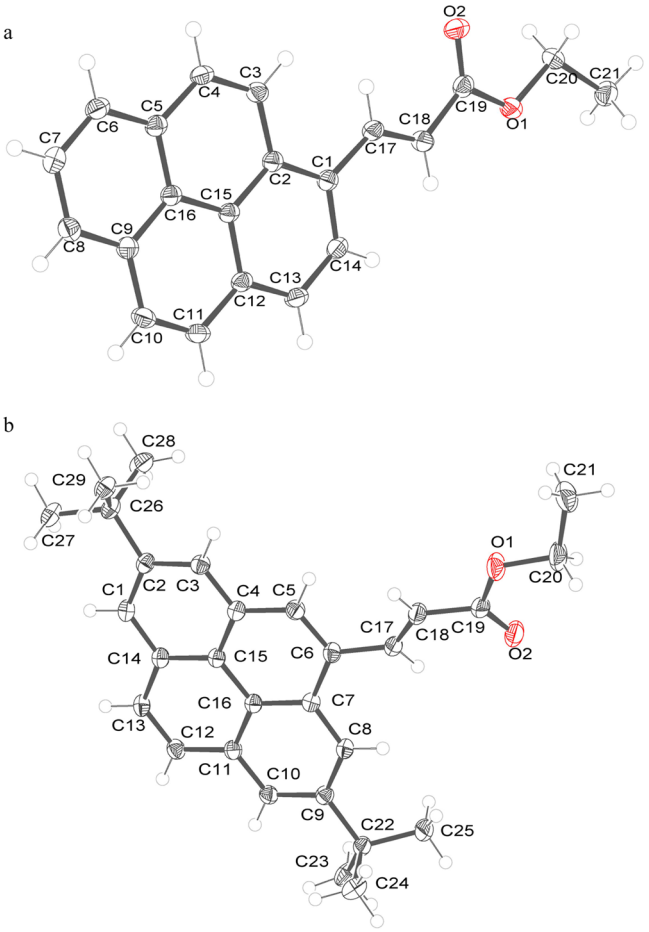

Figure 8. Molecular structure of **2a** (a) and **3b** (b) (ORTEP representation). Displacement ellipsoids were drawn at the 50% probability level (CCDC nos. 102956 and 102957, respectively).

Table 6. Selected Dihedral Angles (deg) for the Structures of 2a and 3b

2a		3b	
C12−C15−C16−C5	−178.97(15)	C14−C15−C16−C7	176.42(11)
C12−C15−C16−C9	0.7(2)	C14−C15−C16−C11	−2.83(18)
C14 −C1−C17−C18	4.3(3)	C5 −C6−C17−C18	26.5(2)
C17−C18−C19−O1	176.54(14)	C17−C18−C19−O1	171.71(13)

molecules in the following stacks along [010] are antiparallel and there are weak C−H···O interactions between the C−H bonds from the pyrene moiety in one stack and the carbonyl oxygen from the molecule in the next stack.

The arrangement of the stacks is best viewed along the [100] direction (Figure 9a), and the structure as a whole is a typical herringbone arrangement (Figure 9b). Extensive stacking enables the formation of dynamic and preformed excimers of **2a** upon excitation in the solid state, which is fully compatible with the time-resolved results that were extensively discussed in the previous paragraphs (see section 2.3).

The molecules of **3b** do not show $\pi-\pi$ stacking in the crystal lattice (Figure 10). Molecules related by the center of symmetry form short C − H ··· π contacts between the C28 methyl group of the C26 *tert*-butyl moiety and the side of the pyrene ring. The interaction is significant, as the C26 carbon of

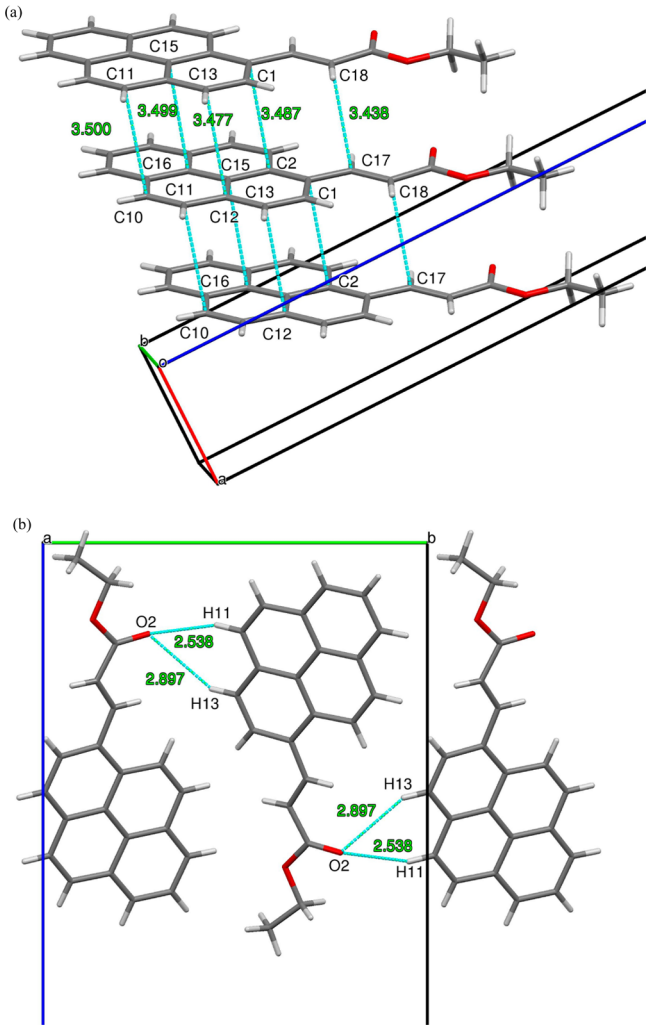

Figure 9. Intermolecular interactions in the crystal structure of **2a**: (a) π-stacking of the molecules along [100]; (b) C−H···O interactions between the molecules from adjacent stacks along [010] direction. The crystallographic *a*,*b*,*c* axes are marked as red, green, and blue, respectively.

the C26 *tert*-butyl moiety is tilted out of the average pyrene plane by 0.2 Å in the direction of the neighboring pyrene moiety (Figure 10a). Such preformed dimers are stacked along the [010] direction (Figure 10b). The methyl groups from the C22 *tert*-butyl moiety, on the other hand, are directed toward the carbonyl group of the side chain, forming relatively short C − H ··· O contacts with the H··· O distance in the range of 2.7−2.9 Å. The structure is additionally stabilized by C − H···π interactions, in particular C12−H12···C11. In contrast to the structure of **2a**, there are no short $\pi-\pi$ intermolecular contacts in which the interatomic distance is short enough to allow the formation of dynamic excimers. Most of the molecules can be described as monomer species, but some dimeric configurations revealed by the crystal structure allow a small proportion of preformed excimers, which is in agreement with the solid state spectroscopic data discussed in the previous part (2.3).

4. CONCLUSION

We demonstrated, using ethyl acrylate as a model alkene, the potential of the dehydrogenative Heck (Fujiwara−Moritani) reaction for the synthesis of alkenyl-substituted pyrenes. The 3-

DOI: 10.1021/jo502619k
J. Org. Chem. 2015, 80, 2573−2581

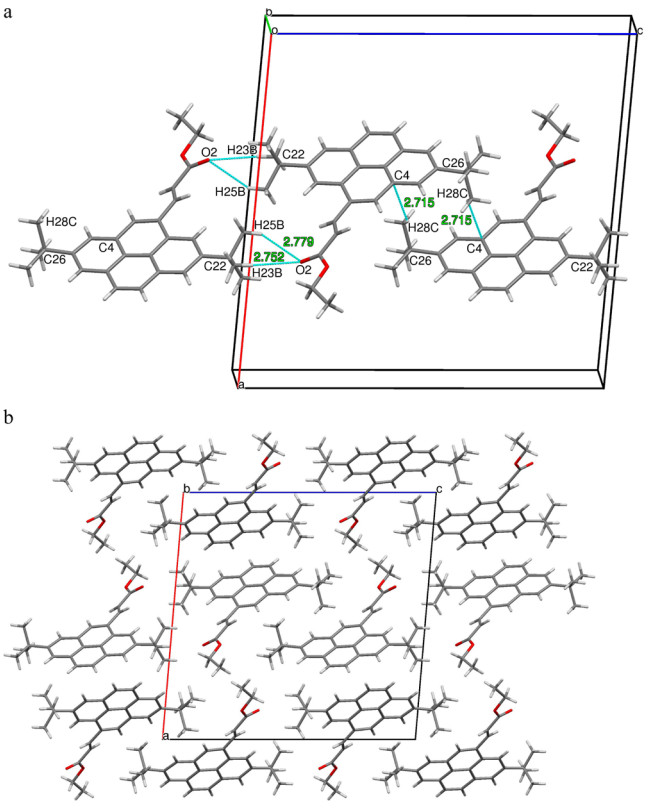

Figure 10. Intermolecular interactions and crystal packing of **3b**: (a) C−H···π and C−H···O interactions viewed approximately along [010] and (b) view along [010]. The crystallographic *a*, *b*, *c* axes marked as red, green, and blue, respectively.

pyrenyl acrylates derivatives synthesized via this route display strong fluorescence in solution and in the solid state. A time-resolved study revealed that in addition to blue emission arising for monomer species in the solid state, green emission was observed originating from aggregated pyrenyl species of **2a** and **3a**,**b** (preformed excimers). Interestingly, in the case of compound **2a**, red-emission was also evidenced due to dynamic excimers formed by efficient $\pi-\pi$ stacking in the solid state and supported by crystallographic data. The variable nature and proportion of emitting species in the solid state leads to fascinating photophysical properties for the **2a** and **3a**,**b** series, with different emission colors and quantum yields.

5. EXPERIMENTAL SECTION

General Procedure for Dehydrogenative Heck Reaction of 1a,b with Ethyl Acrylate. Palladium acetate (5.6 mg, 0.025 mmol) and DAF (9.1 mg, 0.05 mmol) were added to a suspension of **1a** or **1b** (1.5 mmol) in acetic (in the case of **1a**) or pivalic acid (in the case of **1b**) (1.5 mL) containing ethyl acrylate (55 μL, 0.5 mmol). The resulting mixture was heated to100 °C (1a) or 130 °C (**1b**). A gradual dissolution of pyrene was observed along with the appearance of a yellow coloration. After cooling to room temperature the mixture was diluted with chloroform (~100 mL) and the acid was removed by extraction with aq $NaHCO_3$. The solvent was evaporated, and the unreacted pyrene and the product(s) were isolated by column chromatography on silica gel 60 (230−400 mesh) using CH_2Cl_2 as eluent.

*(E)-Ethyl 3-(Pyren-1-yl) acrylate (**2a**).*[10] Yellow solid. Yield (**2a** + **3a**) 71% (0.106 g). Isolated by repeated crystallization from hexanes. Mp: 108−109 °C. R_f = 0.61 (silica gel, CH_2Cl_2). ^{1}H NMR: δ 8.82 (d, J = 15.6 Hz, 1H), 8.46 (d, J = 9.0 Hz, 1H), 8.25 (d, J = 7.8 Hz, 1H), 8.20 (d, J = 7.8 Hz, 2H8.16 (d, J = 9.6 Hz, 1H), 8.12 (d, J = 7.8 Hz, 1H), 8.10 (d, J = 8.4 Hz, 1H), 8.02 (m, 2H), 6.70 (d, J = 15.6 Hz, 1H), 4.37 (q, J = 7.2 Hz, 2H), 1.42 (t, J = 7.2 Hz, 3H). ^{13}C NMR: δ 167.1, 141.3, 132.6, 131.3, 130.7, 129.7, 128.51, 128.48, 128.3, 127.3, 126.2, 125.9, 125.7, 125.0, 124.9, 124.6, 124.2, 122.4, 120.4, 60.6, 14.4. IR (KBr) ν 3051, 2980, 2904, 1709, 1620, 1596, 1318, 1285, 1244, 1168, 843. MS (EI, 70 eV) m/e 300 (58, M^+), 227 (100, M − $COOEt^+$), 226 (82, M − $HCOOEt^+$). Anal. Calcd ($C_{21}H_{16}O_2$): C, 83.98; H, 5.37. Found: C, 83.72; H, 5.41; H, 5.46.

*(E)-Ethyl 3-(2,7-Di-tert-butylpyren-4-yl)acrylate (**3b**).* Pale yellow solid. Yield: 45% (0.093 g). Mp: 159−160 °C. R_f = 0.82 (silica gel 60, CH_2Cl_2). ^{1}H NMR (600 MHz, $CDCl_3$) δ 8.71 (d, J = 15.8 Hz, 1H), 8.46 (d, J = 1.8 Hz, 1H), 8.32 (s, 1H), 8.24 (d, J = 1.8 Hz, 1H), 8.22 (dd, J_1 = 1.8 Hz, J_2 = 4.2 Hz, 2H), 8.03 (dd, J_1 = 9.0 Hz, J_2 = 13.2 Hz, 2H), 6.77 (d, J = 15.6 Hz, 1H), 4.38 (q, J = 7.2 Hz, 2H), 1.60 (s, 9H), 1.59 (s, 9H), 1.42 (t, J = 7.2 Hz, 3H). ^{13}C NMR (150 MHz, $CDCl_3$): δ 167.1, 149.1, 148.9, 142.7, 131.7, 131.2, 130.8, 130.0, 129.0, 127.8, 127.3, 127.2, 123.3, 123.2, 123.0, 122.9, 122.7, 121.2, 118.4, 60.6, 35.5, 35.2, 32.0, 31.9, 14.4. IR (KBr) ν 3042, 2962, 2902, 2868, 1713, 1636, 1625, 1605, 1477, 1459, 1175, 1037, 875. MS (EI, 70 eV) m/e 412 (100, M^+). Anal. Calcd ($C_{29}H_{32}O_2$): C, 84.43; H, 7.82. Found: C, 84.22; H, 7.91.

*(E)-Ethyl 3-(Pyren-4-yl)acrylate (**3a**).* A mixture of 4-bromopyrene (140 mg, 0.5 mmol), ethyl acrylate (110 μL, 1 mmol), $Pd(OAc)_2$ (11 mg, 0.05 mmol), tris(*o*-tolyl)phosphine (30 mg, 0.1 mmol), and potassium carbonate (138 mg, 1 mmol) in dimethylformamide (2 mL) was refluxed for 6 h under argon. The reaction mixture was extracted with chloroform, washed with water, and dried (Na_2SO_4). The solvent was evaporated, and **3a** was isolated by column chromatography on silica gel 60 (230−400 mesh) using dichloromethane as eluent. Pale yellow solid. Yield: 65% (0.098 g). Mp: 114−115 °C. R_f = 0.61 (silica gel 60, CH_2Cl_2). ^{1}H NMR (600 MHz, $CDCl_3$) δ 8.62 (d, J = 15.6 Hz, 1H), 8.41 (d, J = 7.8 Hz, 1H), 8.21 (s, 1H), 8.15 (dd, J_1 = 10.8 Hz, J_2 = 7.2 Hz, 2H), 8.11 (d, J = 7.8 Hz, 1H), 7.99 (m, 4H), 6.71 (d, J = 15.6 Hz, 1H), 4.40 (q, J = 7.2 Hz, 2H), 1.45 (t, J = 7.2 Hz, 3H). ^{13}C NMR (150 MHz, $CDCl_3$) δ 166.8, 142.2, 131.44, 131.36, 130.9, 130.2, 129.2, 127.6, 127.1, 126.6, 126.1, 125.91, 125.86, 125.7, 125.5, 124.8, 124.7, 121.4, 121.2, 60.6, 14.4. IR (KBr) ν 3039, 2979, 2909, 1703, 1636, 1623, 1307, 1192, 1173, 862, 826. MS (EI, 70 eV): m/e 300 (44, M^+), 227 (100, M − $COOEt^+$), 226 (50, M − $HCOOEt^+$). Anal. Calcd ($C_{21}H_{16}O_2$): C, 83.98; H, 5.37. Found: C, 83.87; H, 5.46.

■ ASSOCIATED CONTENT

Ⓢ Supporting Information

Figures giving ^{1}H NMR, ^{13}C NMR, and IR spectra of the products **2a** and **3a**,**b** along with X-ray diffraction analyses of **2a** and **3b**. This material is available free of charge via the Internet at http://pubs.acs.org.

■ AUTHOR INFORMATION

Corresponding Authors

*E-mail: janzak@uni.lodz.pl.

*E-mail: metivier@ppsm.ens-cachan.fr.

Notes

The authors declare no competing financial interest.

■ ACKNOWLEDGMENTS

Financial support from the National Science Centre Poland (NCN, Grant Harmonia UMO-2012/04/M/ST5/00712) is gratefully acknowledged.

■ REFERENCES

(1) Figueira-Duarte, T. M.; Muellen, K. *Chem. Rev.* **2011**, *111*, 7260−7314.

(2) Bains, G.; Patel, A. B.; Narayanaswami, V. *Molecules* **2011**, *16*, 7909−7935.

(3) Yao, C. X.; Kraatz, H. B.; Steer, R. P. *Photochem. Photobiol. Sci.* **2005**, *4*, 191−199.

DOI: 10.1021/jo502619k
J. Org. Chem. 2015, 80, 2573−2581

(4) Ottonelli, M.; Piccardo, M.; Duce, D.; Thea, S.; Dellepiane, G. *J. Phys. Chem. A* **2012**, *116*, 611−630.
(5) Flamholc, R.; Plażuk, D.; Zakrzewski, J.; Métivier, R.; Nakatani, K.; Makal, A.; Woźniak, K. *RSC Adv.* **2014**, *4*, 31594−31601.
(6) Métivier, R.; Leray, I.; Lefevre, J.-P.; Roy-Auberger, M.; Zanier-Szydlowski, N.; Valeur, B. *Phys. Chem. Chem. Phys.* **2003**, *5*, 758−766.
(7) Breul, A. M.; Hager, M. D.; Schubert, U. S. *Chem. Soc. Rev.* **2013**, *42*, 5366−5407.
(8) Ito, F.; Kakiuchi, T.; Sakano, T.; Nagamura, T. *Phys. Chem. Chem. Phys.* **2010**, *12*, 10923−10927.
(9) Sharif, M.; Reimann, S.; Wittler, K.; Knöpke, L. R.; Surkus, A.-E.; Roth, C.; Villinger, A.; Ludwig, R.; Langer, P. *Eur. J. Org. Chem.* **2011**, 5261−5271.
(10) Reimann, S.; Sharif, M.; Wittler, K.; Knöpke, L. R.; Surkus, A. E.; Roth, C.; Ludwig, R.; Langer, P. *Z. Naturforsch. C: Biosci.* **2013**, *68*, 367−377.
(11) Li, Y.-X.; Sun, G.-X.; Miao, J.-L.; Nie, Y.; Zhang, Z.-W.; Tao, X.-T. *Tetrahedron Lett.* **2013**, *54*, 3263−3267.
(12) Sharif, M.; Reimann, S.; Wittler, K.; Knoepke, L. R.; Surkus, A.-E.; Roth, C.; Villinger, A.; Ludwig, R.; Langer, P. *Eur. J. Org. Chem.* **2011**, 5261−5271.
(13) Yang, X. H.; Giovenzana, T.; Feild, B.; Jabbour, G. E.; Sellinger, A. *J. Mater. Chem.* **2012**, *22*, 12689−12694.
(14) Lo, M. Y.; Zhen, C.; Lauters, M.; Jabbour, G. E.; Sellinger, A. *J. Am. Chem. Soc.* **2007**, *129*, 5808−5809.
(15) Lo, M. Y.; Ueno, K.; Tanabe, H.; Sellinger, A. *Chem. Rec.* **2006**, *6*, 157−168.
(16) Le Bras, J.; Muzart, J. *Chem. Rev.* **2011**, *111*, 1170−1214.
(17) Wencel-Delord, J.; Nimphius, C.; Patureau, F. W.; Glorius, F. *Chem.—Asian J.* **2012**, *7*, 1208−1212.
(18) Wencel-Delord, J.; Nimphius, C.; Patureau, F. W.; Glorius, F. *Angew. Chem., Int. Ed.* **2012**, *51*, 2247−2251.
(19) Kuhl, N.; Hopkinson, M. N.; Wencel-Delord, J.; Glorius, F. *Angew. Chem., Int. Ed.* **2012**, *51*, 10236−10254.
(20) Yoo, W.-J.; Li, C.-J. *Top. Curr. Chem.* **2010**, *292*, 281−302.
(21) Guo, X.; Li, Z.; Li, C. *Prog. Chem.* **2010**, *22*, 1434−1441.
(22) Wencel-Delord, J.; Droege, T.; Liu, F.; Glorius, F. *Chem. Soc. Rev.* **2011**, *40*, 4740.
(23) Glorius, F. *Nat. Chem.* **2010**, *2*, 78−80.
(24) Bugaut, X.; Glorius, F. *Angew. Chem.Int. Ed.* **2011**, *50*, 7479−7481.
(25) Mochida, K.; Kawasumi, K.; Segawa, Y.; Itami, K. *J. Am. Chem. Soc.* **2011**, *133*, 10716−10719.
(26) Kawasumi, K.; Mochida, K.; Kajino, T.; Segawa, Y.; Itami, K. *Org. Lett.* **2011**, *14*, 418−421.
(27) Liu, Z.; Wang, Y.; Chen, Y.; Liu, J.; Fang, Q.; Kleeberg, C.; Marder, T. B. *J. Org. Chem.* **2012**, *77*, 7124−7128.
(28) Coventry, D. N.; Batsanov, A. S.; Goeta, A. E.; Howard, J. A. K.; Marder, T. B.; Perutz, R. N. *Chem. Commun.* **2005**, 2172−2174.
(29) Piotrowicz, M.; Zakrzewski, J.; Makal, A.; Bak, J.; Malińska, M.; Woźniak, K. *J. Organomet. Chem.* **2011**, *696*, 3499−3506.
(30) Konieczny, M.; Harvey, R. G. *J. Org. Chem.* **1979**, *44*, 2158−2160.
(31) Yamato, T.; Fujimoto, M.; Miyazawa, A.; Matsuo, K. *J. Chem. Soc., Perkin Trans. 1* **1997**, 1201−1207.
(32) Rodenburg, L.; Brandsma, R.; Tintel, C.; Cornelisse, J.; Lugtenburg, J. *J. Chem. Soc., Chem. Commun.* **1983**, 1039−1039.
(33) Hu, J. Y.; Paudel, A.; Yamato, T. *J.Chem. Res.* **2009**, 109−113.
(34) Min, M.; Hong, S. *Chem. Commun.* **2012**, *48*, 9613−9615.
(35) Min, M.; Choe, H.; Hong, S. *Asian J. Org. Chem.* **2012**, *1*, 47−50.
(36) Liégault, B.; Lee, D.; Huestis, M. P.; Stuart, D. R.; Fagnou, K. *J. Org. Chem.* **2008**, *73*, 5022−5028.
(37) Winnik, F. M. *Chem. Rev.* **1993**, *93*, 587−614.
(38) Zhao, Z.; Chen, S.; Lam, J. W. Y.; Wang, Z.; Lu, P.; Mahtab, F.; Sung, H. H. Y.; Williams, I. D.; Ma, Y.; Kwok, H. S.; Tang, B. Z. *J. Mater. Chem.* **2011**, *21*, 7210−7216.
(39) Katoh, R.; Suzuki, K.; Furube, A.; Kotani, M.; Tokumaru, K. *J. Phys. Chem. C* **2009**, *113*, 2961−2965.
(40) Seko, T.; Ogura, K.; Kawakami, Y.; Sugino, H.; Toyotama, H.; Tanaka, J. *Chem. Phys. Lett.* **1998**, *291*, 438−444.

DOI: 10.1021/jo502619k
J. Org. Chem. 2015, 80, 2573−2581